JOURNAL OF GEOPHYSICAL RESEARCH, VOL. 106, NO. D18, PAGES 20,629–20,639, SEPTEMBER 27, 2001

Surface stress in offshore flow and quasi-frictional decoupling

L. Mahrt,[1] Dean Vickers,[1] Jielun Sun,[2] Timothy L. Crawford,[3]
Gennaro Crescenti,[3] and Paul Frederickson[4]

Abstract. Aircraft data collected at approximately 15 m above the sea surface in the coastal zone are analyzed to examine the spatial distribution of surface stress. Advection of stronger turbulence from land dominates the near-surface turbulence for the first few kilometers offshore. With offshore flow of warm air over cold water, strong stratification leads to very small surface stress. Because the stability restricts the momentum transfer to the waves, the aerodynamic surface roughness decreases to very small values, which in turn decreases atmospheric mixing. The redevelopment of the boundary layer farther downstream is examined. Computation of fluxes from observations for stable cases is difficult due to a variety of errors including large random flux errors, possible instrumental loss of small-scale flux, difference between the surface flux and that at the observational level, and inadvertent capture of mesoscale motions in the computed turbulent fluctuations. Although the errors appear to be substantial, the aircraft momentum fluxes compare favorably with those from sonic anemometers on two buoys and a tower at the end of a 570-m pier, even with near collapse of the turbulence.

1. Introduction

Existing models of the air-sea interaction sometimes break down in the near-coastal zone due to advection of stronger turbulence and temperature from land, nonstationarity associated with diurnally varying horizontal pressure gradients in the atmosphere, complex wave states, including young wind-driven waves and incoming swell, and shoaling of such swell. A number of studies have formulated transfer coefficients in terms of fetch [*Perrie and Toulany*, 1990] or wave age [e.g., *Geernaert et al.*, 1987; *Toba and Koga*, 1986; *Maat et al.*, 1991; *Vickers and Mahrt*, 1997a].

Advection of stronger turbulence from land can strongly influence the air-sea interaction in offshore flow [*Mahrt et al.*, 2001; *Vickers et al.*, 2001]. Some of the perceived dependence on wave age in offshore flow, whether based on friction velocity or wind speed, may be due to the influence of advection of stronger turbulence from the land surface, which decays in the downstream direction and influences the drag coefficient in a manner similar to the wave age dependence [*Sun et al.*, 2001]. This advection links the fluxes over the sea with the characteristics of the upstream land surface. *Winstead and Young* [2000] and N. Winstead and P. Mourad (Shallow great lakes scale atmospheric thermal circulation imaged by synthetic aperture radar; submitted to *Monthly Weather Review*, 2001) find that alongshore variation of land characteristics (farmland, woods, and towns) leads to alongshore variation of high-frequency surface wave energy in offshore flow; more wave energy is generated downstream from rougher land surfaces.

With offshore flow of warm air over cool water, the turbulence and surface stress can become suppressed by the stratification, referred to as quasi-frictional decoupling by *Smedman et al.* [1997a, 1997b], perhaps analogous to development of the very stable nocturnal boundary layer over land. Over land, surface cooling and stratification of the air near the surface reduces turbulence and downward heat flux, which leads to stronger net cooling of the surface and further enhancement of the stratification. Over the water the surface temperature is more constant, but the reduction of downward momentum flux by the stratification reduces generation of the surface wave field, which in turn reduces the surface roughness [*Plant et al.*, 1998] and subsequently reduces mechanical generation of atmospheric turbulence. Over land the roughness length is normally considered to be a constant for a given location and wind direction.

The partial collapse of turbulence in offshore flow of warm air over cooler water is emphasized in this study because it is the case most poorly simulated by existing models. On the basis of observations in the coastal zone in the Baltic Sea, *Smedman et al.* [1997b] find that the atmospheric boundary layer over the Baltic Sea is stable more often than unstable and the influence of warm air advection from land can extend 150 km offshore. In this study, offshore flow will be examined in terms of eddy correlation aircraft data collected approximately 15 m above the sea surface (section 3). In the next section we review the basic formulations required for the analysis in sections 4–7, using the data described in section 3.

2. Existing Parameterization of the Surface Stress

The drag coefficient is computed as

$$C_d = \frac{u_*^2}{\overline{U^2}}, \tag{1}$$

where u_* is the friction velocity based on averaged components of the stress vector and U is the wind speed computed from

[1]College of Oceanic and Atmospheric Sciences, Oregon State University, Corvallis, Oregon, USA.
[2]National Center for Atmospheric Research, Boulder, Colorado, USA.
[3]NOAA Air Resources Laboratory, Idaho Falls, Idaho, USA.
[4]Naval Postgraduate School, Monterey, California, USA.

Paper number 2000JD000159.
0148-0227/01/2000JD000159$09.00

averaged wind components. Given observations of the wind speed and surface stress, the roughness length can be "backed out" of the similarity prediction of the drag coefficient.

$$C_d = \left[\frac{\kappa}{\ln (z/z_o) - \psi_m}\right]^2, \quad (2)$$

where z is the observational level, z_o is the roughness length for momentum, κ is the von Karmen constant, taken as 0.4, and ψ_m is a function of the stability z/L, where L is the Obukhov length, expressed as

$$L = -\frac{u_*^3}{(\kappa g/\theta_v)([w'\theta'] + 0.61\theta[w'q'])}, \quad (3)$$

where θ is the potential temperature and q is the specific humidity. The stability function will be computed from *Paulson* [1970] for unstable conditions and from *Dyer* [1974] for stable conditions.

Using (2), the aerodynamic roughness length z_o can then be estimated from the observed values of u_*, U, and L and the specified function ψ. The computed roughness lengths could include compensation for incorrect stability functions ψ. However, Monin-Obukhov similarity theory was found to be a good approximation for the flux-gradient relationship in quasi-stationary homogeneous flow over the sea in terms of the turbulence energy budget [*Edson and Fairall*, 1998; *Wilczak et al.*, 1999] and flux-gradient relationship [*Vickers and Mahrt*, 1999], although modest adjustments of the stability function were suggested in the later study. The dependence of the roughness length on stability is equivalent to a dependence of the neutral drag coefficient on stability. Often the drag coefficient is reduced to a neutral value to remove the influence of stability. The neutral drag coefficient may exhibit a dependence on stability, which is sometimes interpreted as failure of Monin-Obukhov similarity theory or a failure of the existing stability functions. However, the reduction of the drag coefficient to neutral conditions assumes either constant roughness length or the Charnock formulation [*Charnock*, 1955] with constant coefficient. Both assumptions may be incorrect and are not a part of Monin-Obukhov similarity theory. Therefore a stability-dependent roughness length is not necessarily an indicator of the failure of Monin-Obukhov similarity theory.

3. Data and Analysis

Surface fluxes are estimated for the Shoaling Waves Experiment (SHOWEX) in October–November 1997 and March 1999 and in November–December 1999 [*Sun et al.*, 2001; *Crescenti et al.*, 1999; *French et al.*, 2000] using the low-level aircraft data from 37 flights on 35 days at an average height 15 m above the sea surface. The data were collected by the LongEZ research aircraft over Atlantic coastal water off the Outer Banks near Duck, North Carolina. The SHOWEX data have minimal instrumentation problems compared with the previous two field programs and several improvements in preprocessing and will be emphasized in this study.

For both experiments in 1999, a Campbell CSAT sonic anemometer (10-cm path length) operated at approximately 18 m above the water on a tower at the end of a 570-m pier (U.S. Army Corps of Engineers Field Research Facility). In November–December 1999 a second CSAT sonic anemometer was deployed on a 3-m boom attached to the top of the railing at the end of the pier, 8 m above the sea surface. To avoid serious flow distortion, we include only those time periods with winds from the northerly sector between 295 and 70 degrees for the northward pointing sonic anemometer on the rail, and easterly flow between 360 and 180 degrees for the eastward pointing 18-m sonic on the tower. Smoke releases indicated that the distortion due to the pier for the accepted wind directions did not extend to the end of the 3-m boom, which is consistent with the close agreement between the fluxes computed from the 18- and 8-m sonic anemometers. Both the aircraft and sonic anemometer data were subjected to quality control procedures similar to those described by *Vickers and Mahrt* [1997b].

3.1. Flight Pattern and Analysis Strategy

Thirteen flights from the three experiments measured horizontal and vertical structure in the lowest few hundred meters above the sea surface in the first 10–20 km offshore. Other types of flight patterns include a series of flight tracks parallel to the shore, box patterns, 100-km transects perpendicular to the coast, and a few mission-specific patterns. For the analyses in sections 4–7, all flights are used that collected low-level data over the Atlantic side of the Outer Banks with a fetch greater than 10 km for offshore flow.

3.2. Vertical Flux Divergence

Smedman et al. [1997a, 1997b] point out that the boundary layer may be very thin in stable conditions over the sea and that standard observational levels may be too high to estimate surface fluxes. Even though the LongEZ generally flew about 15 m above the sea surface, the difference between the flux at this level and the sea surface stress may be significant in thin boundary layers or advective conditions. The difference between the stress at the aircraft level and the sea surface is constrained by the equation of motion. Integrating the equation of motion for the offshore flow component between the surface and the aircraft level, z, for stationary flow, the surface stress is

$$\overline{w'u'}_{sfc} = \overline{w'u'}_z - \int_{sfc}^{z}\left[\bar{u}\frac{\partial\bar{u}}{\partial x} + \bar{w}\frac{\partial\bar{u}}{\partial z} + \frac{\partial\overline{u'^2}}{\partial x}\right]dz + \int_{sfc}^{z} f(\bar{v} - V_G)\,dz, \quad (4)$$

where we have neglected derivatives parallel to the coast (here the y direction), f is the Coriolis parameter, and V_G is the geostrophic wind. The difference between the momentum flux at the sea surface and at the observational level $z \approx 15$ m is constrained by the magnitude of the advection, horizontal flux divergence, and the ageostrophic term (the last term on the right-hand side).

Vickers et al. [2001] find that within the first few kilometers downstream from the coast, strong horizontal advection of weaker momentum is partially balanced by vertical convergence of the downward turbulent momentum flux and downward advection of stronger momentum by mean subsidence. The subsidence is associated with acceleration of offshore flow. On the basis of x-z cross-section analysis of the stress in stable offshore flow using multiple aircraft levels, *Vickers et al.* [2001] found the surface stress to be typically of the order of 10^{-2} m^2 s^{-2} smaller than the stress at the 15-m aircraft level in the first few kilometers of offshore flow. This difference can be more than 30% of the absolute flux value.

Farther offshore, advection terms become small but the depth of the turbulence might be very thin (section 6). Then

the stress divergence between the aircraft level and the surface is supported by the large-scale ageostrophic flow $f(\bar{v} - V_G)$, which is expected to be of the order of 10^{-4} m s^{-2}. This value corresponds to a change of stress of 1.5×10^{-3} m^2 s^{-2} between the surface and the aircraft level. This value is only a little smaller than the smallest stress values observed in stable offshore flow (section 4) and therefore could be important. That is, the stress at 15 m might be significantly smaller than that at the sea surface.

The influence of the height of the platform on the computed roughness length will be an important concern in this study. The height of the aircraft for low-level flights included here ranged from roughly 10 m to a specified upper cutoff of 20 m. Roughness lengths computed from the aircraft data within this range of heights do not show a clear dependence on the height of the aircraft. Comparison of the two levels of momentum and heat flux measurements at the end of the pier for onshore flow shows good agreement. However, the computed roughness length is systematically smaller at the 18-m level. This appears to be due to the increase of wind speed with height faster than predicted by similarity theory. Perhaps the 18-m level is often above the surface layer, which would also imply that the aircraft was sometimes above the surface layer.

3.3. Variable Averaging Length

In this study the dependence of the fluxes on averaging scale is studied in terms of multiresolution cospectra [e.g., *Howell and Mahrt*, 1997], which can be thought of as a wavelet decomposition using unweighted averaging lengths of different (dyadic) lengths as the local basis set. Interpretation of such cospectra does not require the assumption of periodicity, and the properly integrated multiresolution cospectra exactly satisfy Reynolds averaging.

For very stable conditions, fluxes can be quite small and confined to small horizontal scales, less than 100 m. As a result, the usual use of a 1-km window may capture significant nonturbulent mesoscale flux, which can be primarily flux sampling errors. Normally, this mesoscale flux is small compared with the turbulent flux. However, with very stable conditions, the turbulent flux is small, and the mesoscale scale flux may even dominate the computed flux. Therefore we have used a smaller averaging window to define perturbations for very stable conditions. The averaging length is determined separately for each 5-km record based on an empirical relationship (constructed below) between the averaging length and the bulk Richardson number,

$$Rb = \frac{g}{\theta} \frac{\delta\theta z}{U^2}, \tag{5}$$

where $\delta\theta$ is the difference of potential temperature between the aircraft level and the sea surface. The bulk Richardson number is used instead of z/L, since the later is a stronger function of the averaging length itself. The sea surface temperature measured from the LongEZ was calibrated using buoy measurements for each flight day.

The length scale associated with the gap region separating turbulence and mesoscale transport is estimated from cospectra of momentum, heat, and moisture for individual flights (Figure 1). A gap scale was identified when the slope of the cospectra changed sign or when the cospectra crossed zero for length scales exceeding an arbitrary threshold of 100 m. For most flights the gap scales identified for each of the three

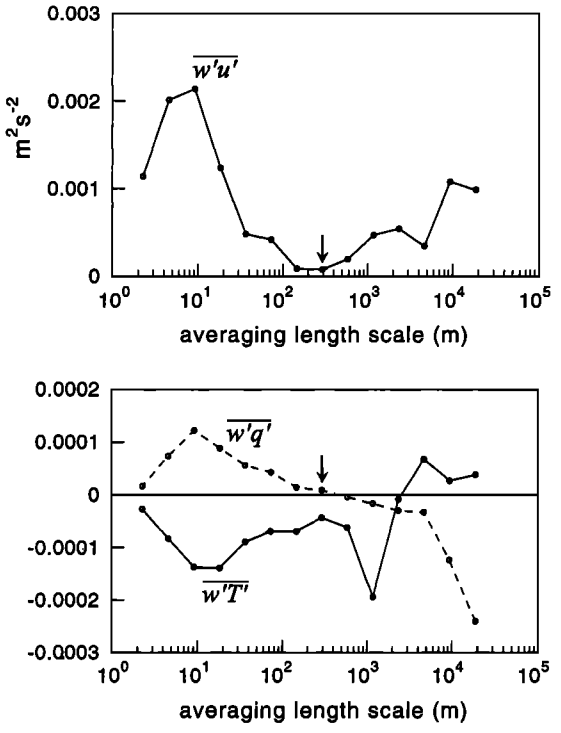

Figure 1. Determination of the averaging length based on the cospectral gap or cospectral sign reversal (vertical arrow) for (a) momentum flux (m^2 s^{-2}), and (b) heat flux (m s^{-1} °C) (solid line) and moisture flux (m s^{-1} g kg^{-1}) (dashed line) in stable conditions for a single aircraft pass on November 21.

cospectra were approximately equal. When the gap scales for the momentum, heat, and moisture fluxes were not the same, we chose an average value even though the gap scale often seemed better defined for moisture where the cospectra typically changed sign in the gap region (cospectral zero crossing).

The values of the gap scale, averaged for different intervals of Rb (Figure 2), were fit to a simple model where horizontal length scale decreases from near 5 km for unstable conditions to only 100 m for very stable conditions (Figure 2). The fluxes based on deviations from the stability-dependent averaging

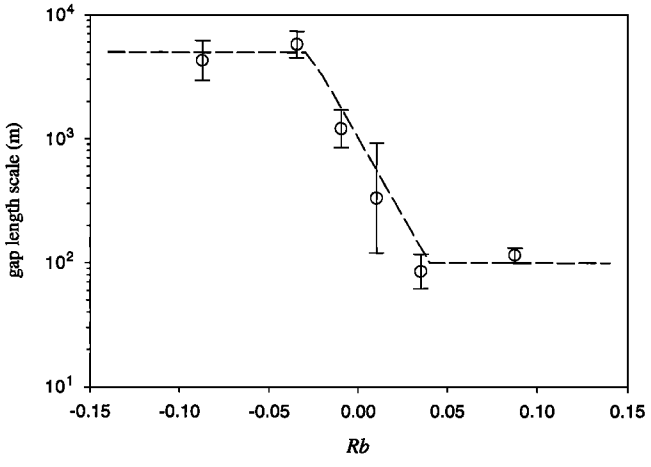

Figure 2. Dependence of the flux averaging length on the bulk Richardson number for bin-averaged values (circles) with the standard error indicated by vertical brackets, and the simplified model fit (dashed line).

length are then averaged over 5-km segments to reduce random flux errors. Application of the variable averaging length tends to increase the fluxes in unstable conditions, on average, and decrease fluxes in stable conditions, on average. However, this systematic change is small, and application of the variable averaging length does not influence the qualitative conclusions of sections 4–7. The most significant change is a reduction of heat flux for stable conditions; however, this changes the log of the roughness length by less than 10%, on average.

3.4. Other Flux Computation Problems

The aircraft data were collected at 50 samples s^{-1} with an air speed of about 55 m s^{-1}, corresponding to a sample interval of about 1 m. Fluxes on horizontal scales smaller than 2 m are lost. This small-scale flux is expected to be missing since the data were low-pass filtered to remove noise at smaller scales. As a result, there is no folding back of small-scale flux to lower frequencies via aliasing. In semicollapsed situations the cospectra do not decrease to small values at the smallest resolvable scale of about 2 m. This implies that momentum flux occurs at even smaller scales. In fact, in a few cases, the cospectra appeared to peak at scales less than 10 m!

As a measure of potential flux loss, we examined the ratio of the flux at the smallest dyadic scale of the multiresolution cospectra to the total flux. With no small-scale flux loss, this ratio should be small. For the momentum flux this ratio increases with stability as the transporting eddies shift to smaller scales, averaging 10% for very stable conditions.

In addition, significant heat flux may be lost for very stable conditions due to the response time of the thermistor, which corresponds to a horizontal scale of 3–4 m. The cospectra of the heat flux tends to vanish at the smallest resolvable scale because the sensor could not resolve variations on this scale. Greater heat flux loss compared with the momentum flux loss causes the estimated stability z/L to be too small. For stable conditions this error acts to underestimate the stability function and therefore to underestimate the roughness length computed from (2). In subsequent sections we use fluxes where no attempt was made to correct for small-scale flux loss, which is under further investigation.

Fluctuations of the aircraft height above the surface, typically of the order of a few meters on a horizontal scale of a kilometer, lead to artificial fluctuations in the presence of mean vertical gradients. The corresponding error for the momentum flux is normally small for unstable conditions. It is large for individual stable records but is not systematic (it occurs with either sign with equal probability) except for very stable conditions, where it acts to overestimate the momentum flux, on average, by 40–50%. The corresponding error in the heat flux is very small. The net effect is to underestimate z/L and the aerodynamic roughness length. Analysis of such errors is complicated and will be reported on in a future paper. Finally, the aircraft may overestimate the wind speed in weak wind conditions, causing the drag coefficient and roughness length to be underestimated.

While the above flux uncertainties seem complex and serious, the aircraft fluxes did compare well with one week of fluxes acquired by the Naval Postgraduate School flux buoy located 10.5 km off the coast (Duck) in 23 m of water (see Figure 5, section 5.1). The LongEZ flew four flights over the buoy during the first week of March 1999. The fluxes from the LongEZ and buoy agreed within the random flux error. On March 2 and 4 the surface friction velocity was small, approximately 0.1 m s^{-1} for both platforms. Stress values from the aircraft data also agree reasonably well with measurements from sonic anemometers mounted on buoys and a sonic anemometer on an offshore tower during SHOWEX (section 5.1). Agreement between instruments does not necessarily imply accurate fluxes since all of the above platforms may underestimate the flux in stable conditions.

Computation of the roughness lengths using Monin-Obukhov similarity theory may be inapplicable if the stress does not approximately oppose the wind. The stress direction may be altered by swell. The influence of swell for weak wind conditions [*Smedman et al.*, 1999; *Grachev and Fairall*, 2001] can cause upward momentum flux from the wave field to the atmosphere, in which case the aerodynamic roughness length has no meaning. In the subsequent analyses we eliminate data where the stress direction deviated by more than 45 degrees from the vector opposite the wind direction. This condition leads to a reduction of the averaged roughness length for weak wind speeds (section 7).

4. Near-Coastal Zone

To organize the discussion, we define three offshore zones for the flow of warm air over cold water: The first is the near-coastal zone, where the stress and roughness length decrease rapidly with fetch in the first few kilometers offshore for stable conditions (Figure 3, solid lines); the second is the quasi-frictional decoupling zone (section 5), where the stress and roughness length maintain extremely small values, often for more than 20 km offshore; the third is the recovery zone, where the stress and roughness length increase, sometimes abruptly (section 6).

Vickers et al. [2001] found that in the first few kilometers offshore, vertical convergence of the downward momentum flux acts to accelerate the flow in the downstream direction. At a fixed point the flow is relatively stationary. The vertical transport of turbulence energy for short fetch is also downward (Figure 4). This downward transport contrasts with the normal concept of a boundary layer, where the vertical transport of turbulence energy is either upward or small. Here this downward transport of turbulence is expressed in terms of the vertical velocity variance since the horizontal velocity variances are more sensitive to choice of averaging length. The vertical transport of the vertical velocity variance ($\overline{w'^3}$) is upward for all of the unstable cases and significantly downward for four of the seven stable cases.

Downstream from the coast the roughness length is expected to increase with wave age (C_p/u_*) with very young wind-driven waves due to increasing amplitude of the waves, until a wave age of 5–10 [e.g., *Nordeng*, 1991], where C_p is the phase speed of the dominant wave. As the wave age increases further, the roughness length decreases due to increasing phase speed of the wind-driven waves and reduction of the relative flow over the waves. The initial stage of increasing stress with increasing fetch, due to wave initiation, is not observed in our data because of the greater influence of advection of turbulence from land [*Sun et al.*, 2001]. Beyond this conclusion, effects of wave state and advection of stronger turbulence from land are difficult to isolate. The advection of stronger turbulence from land can lead to greater downward transport of momentum over the sea, which presumably enhances wave growth, just downstream from the coast.

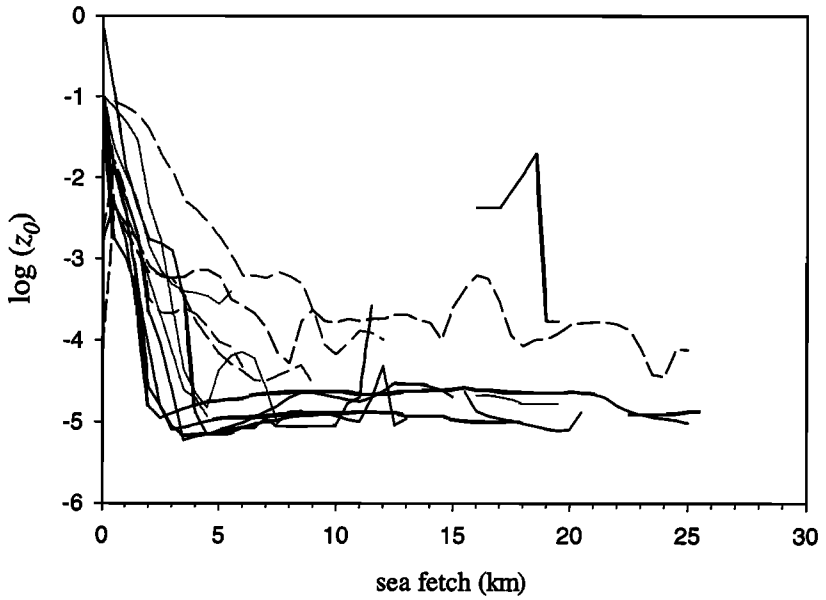

Figure 3. The roughness length as a function of fetch based on heat and momentum fluxes extracted from the 10-m level of the cross-section analyses (section 3.1) for unstable (broken lines) and stable (solid lines) conditions. To remove some extremely small values of roughness lengths and restrict the vertical range of the plot, the roughness length is not allowed to decrease below the smooth flow value (for this plot only). This condition accounts for leveling off of the roughness length in stable cases beyond a fetch of a few kilometers.

5. Quasi-frictional Decoupling Zone

In flow of warm air over cooler water, the stress, turbulence energy, and roughness length decrease by orders of magnitude in the first few kilometers offshore (Figure 3), as opposed to near-neutral and unstable conditions, where they decrease much more slowly. Therefore the stability over the water affects the rate of decrease of the turbulence downstream from the coast. The reduction of downward momentum transfer by the atmospheric stability restricts wave generation and causes very small surface roughness lengths (Figure 3), as previously noted by *Plant et al.* [1998]. These very small surface roughness lengths, in turn, lead to weaker turbulent mixing, and so forth. With such "quasi-frictional decoupling" [*Smedman et al.*, 1997b], the observed aerodynamic roughness length decreases to values several orders of magnitude smaller than the smooth flow value, as also found here. In this study we will loosely refer to quasi-frictional decoupling as cases where the computed roughness length becomes comparable to or substantially less than the smooth flow value. While we recognize that the roughness length may be significantly underestimated (section 3), these conditions correspond to very weak turbulence and values of the friction velocity significantly less than 0.1 m s^{-1}.

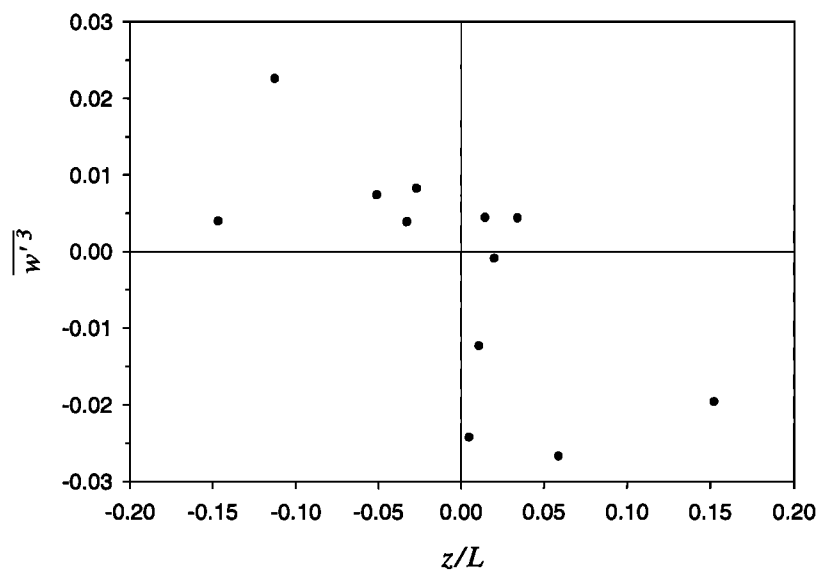

Figure 4. The vertical transport of vertical velocity variance, averaged over the first 2 km offshore as a function of stability.

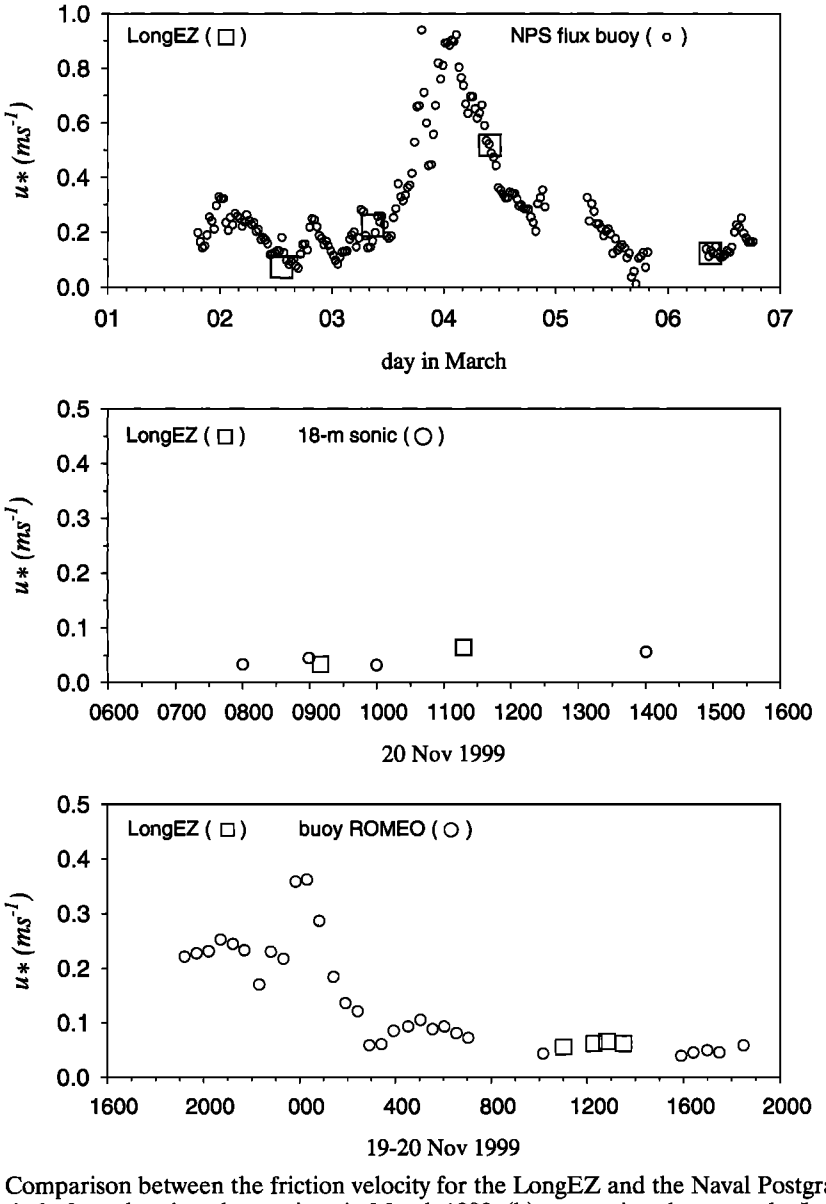

Figure 5. (a) Comparison between the friction velocity for the LongEZ and the Naval Postgraduate School buoy for the period of overlapping observations in March 1999, (b) comparison between the LongEZ friction velocity and that for the 18-m sonic anemometer on November 20, 1999, and (c) comparison between the LongEZ friction velocity and that for buoy Romeo on November 20, 1999.

These small values imply that the flow at the observational level is not fully coupled to the surface in the sense of the usual atmospheric boundary layer.

Here the quasi-frictional decoupling at the observational level begins with travel times typically of the order of 10 min, generally corresponding to fetches greater than 3–5 km (Figure 3), depending on wind speed and upstream turbulence over the land. Even though z/L is significant positive, the buoyancy flux can be relatively small because u_* is small.

5.1. Ultrasmooth

Donelan [1990, p. 265] also calls attention to extremely small roughness lengths referred to as "ultrasmooth" conditions. Variations of surface tension and only small differences between the dominant wave phase speed and wind speed were cited as possible causes. The latter does not appear to be the cause near the coast in this study, where the wind-driven waves are young and the swell opposes the offshore flow. It must be remembered that the aerodynamic roughness length is computed using the stability functions (section 2) and as such does not necessarily have a definable relation to wave state. In other terms, ultrasmooth values of the aerodynamic roughness length do not necessarily imply glassy seas.

While observational errors are large for cases of weak fluxes (section 3), sonic anemometer data show a similar semicollapse of the turbulence. Sonic anemometer measurements at the end of the 570-m pier can be used only with onshore flow where the influence of flow distortion from the tower and the pier is minimized. On November 20, 1999, the flow was weak onshore, with a stable air-sea temperature differences of about 1°C. On this day the friction velocity from the tower (Figure 5b), the buoy Romeo (Figure 5c) (provided by W. Drennen), and the aircraft all show small friction velocity values of approximately 0.05 m s^{-1}. Good agreement is also shown be-

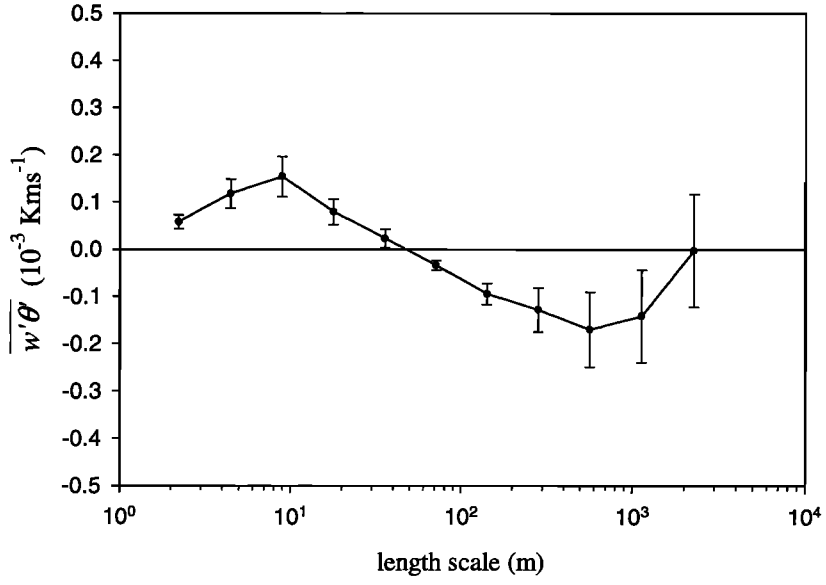

Figure 6. Kinematic heat flux as a function of horizontal scale composited for the seven passes for November 20, 1999. The vertical brackets indicate the standard error based on the between-pass variability for the seven passes.

tween the LongEZ friction velocity and that from the Naval Postgraduate School buoy [*Frederickson and Davidson*, 2000] for the overlap period in March of 1999 (Figure 5a), including a semicollapsed period. We conclude that the surface stress is extremely small but cannot categorically conclude ultrasmooth conditions because of potentially significant flux errors.

The cospectra on this day systematically show upward heat flux at horizontal scales smaller than 50 m and downward heat flux at larger scales (Figure 6). Apparently, the initial overturning corresponds to downward heat flux which destabilizes the flow (cold air on top of warm air). This destabilization leads to upward heat flux by smaller-scale eddies. *Piccirillo and Van Atta* [1997] also find upward buoyancy flux on smaller scales and downward buoyancy flux on larger scales in a stratified wind tunnel with shear. This small-scale upward heat flux was not a systematic condition for stable conditions in SHOWEX.

5.2. Minimum Wind Speed

With offshore flow of air several degrees warmer than the sea surface temperature, ultrasmooth roughness lengths are computed from the present data even for 15-m wind speeds exceeding 10 m s^{-1}. For example, on March 18, 1999, the wind speed reached 12 m s^{-1} while the friction velocity and standard deviation of the vertical velocity both fell below 0.1 m s^{-1}, corresponding to values of the roughness length smaller than the smooth flow value.

This finding for very stable conditions contrasts with the literature where the minimum wind speed for generation of surface waves is considered to be much smaller. The smooth flow regime is often thought to occur, on average, when the wind speed is less than 2.8 m s^{-1} [*Kitaigorodski and Donelan*, 1984] although smooth flow viscous effects can be important up to wind speeds of about 7.5 m s^{-1}. *Kahma and Donelan* [1987] report a range of minimum wind speeds between 0.4 and 5.5 m s^{-1} for initiation of capillary-gravity waves in a laboratory environment. On the basis of radar backscatter, the minimum wind speed for generation of surface waves is estimated to be in the range from 1.0 to 2.0 m s^{-1} [*Moller et al.*, 2000; *Plant et al.*, 1999], although a variety of observational errors for weak wind conditions have been noted [*Moller et al.*, 2000; *Freilich and Dunbar*, 1999; *Weissmann and Graber*, 1999].

6. Recovery Zone

Theoretically, one might expect slow recovery from quasi-frictional decoupling, induced by gradual development of the wave field responding to the weak surface stress, and gradual reduction of the stratification near the surface as the air-sea temperature difference decreases downstream. However, in practice, spatial variation of the sea surface temperature and wind field seem to be more important on a given day, and the recovery from quasi-frictional decoupling seems to assume a different form for each available case. The recovery can take the form of a sudden redevelopment of turbulence, and the turbulence may collapse again farther downwind. However, for most of the cases, the turbulence did not recover within the observational domain, typically extending to 10–20 km from the coast.

For example, the roughness length is still at the smooth flow value, or smaller, at 20-km fetch for four of the five cases of offshore stable flow with complete data coverage out to 20 km (Figure 3). The fifth case, on March 6, 1999, indicates rapid enhancement of the roughness length at 15–20 km offshore. This recovery to large roughness lengths is characterized by downward transport of turbulence energy from higher levels. The latter suggests that the turbulence originates from instability above the thin, cool marine layer and then is transported downward toward the surface. Perhaps the generation of this turbulence is associated with the acceleration of the decoupled flow and enhanced shear above the thin, cool marine layer.

Only limited information is available on the vertical structure in the recovery zone. On November 3, 1997, the flight plan was devoted to sampling the vertical structure of the boundary layer through numerous slant soundings from the coast out to 100 km. On this day the flow was offshore and slightly warmer

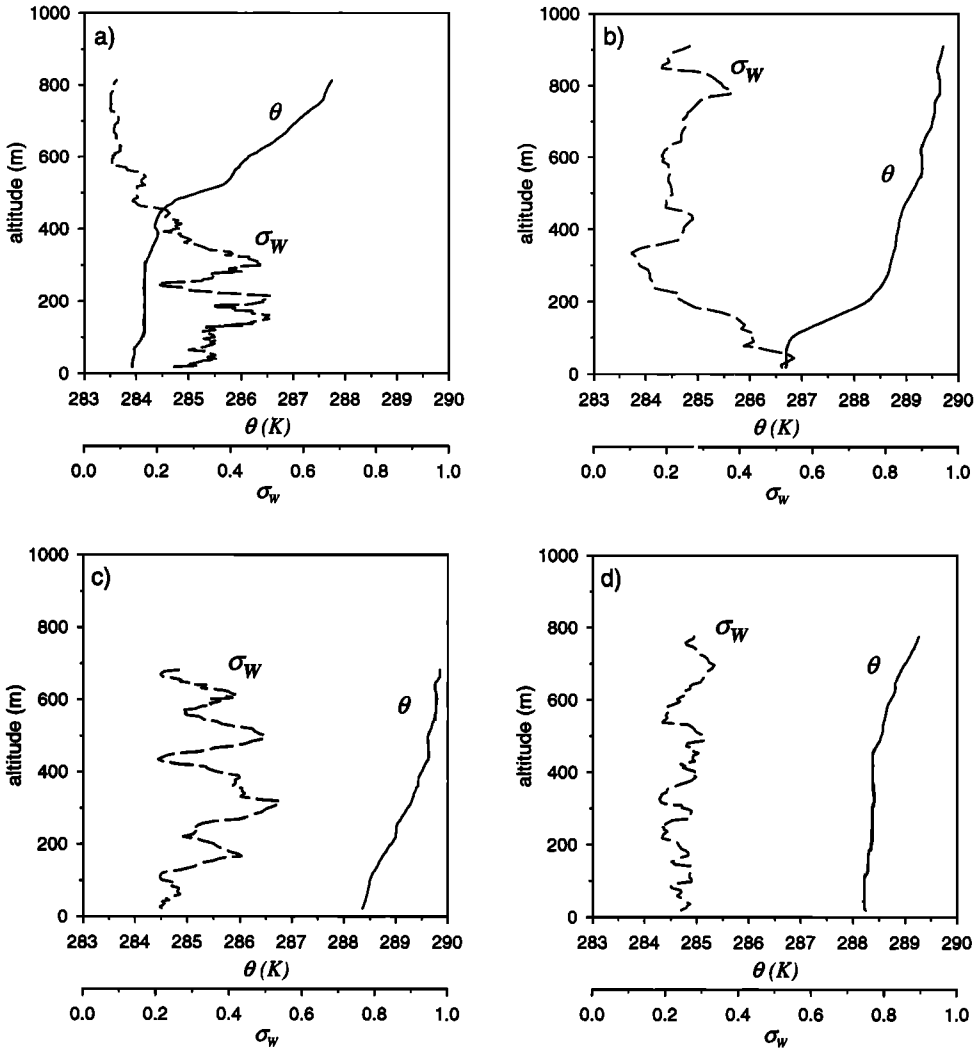

Figure 7. Example slant aircraft soundings of potential temperature and the standard deviation of vertical velocity for November 3, 1997.

than the sea surface. The standard deviation of vertical velocity constructed from slant soundings is noisy because of inadequate sampling at a given level and because of contamination of the computed perturbations by variations of the mean flow within the averaging window of 1 km, as the aircraft ascends and descends. Such errors artificially prevent the standard deviation of vertical velocity from reaching very small values. With a typical ascent rate of 2%, the 1-km averaging length corresponds to a vertical elevation change of 20 m. The sequential soundings indicate a variety of boundary layer structures, and the boundary layer is sometimes poorly defined. The thin, cool boundary layer is observed in only some of the soundings and in other cases may be confined to below the lowest observation level of about 30 m. A few examples are included in Figure 7. Figure 7a shows a deep 400-m boundary layer, while Figure 7b shows a thinner, well-defined boundary layer with significant turbulence over a depth of 100 m. Figure 7d might correspond to a deep boundary layer, while the boundary layer cannot be readily defined in Figure 7c.

Surprisingly, the vertical structure did not seem to vary systematically with offshore distance, suggesting more than one collapse and recovery sequence. The stability on this day is substantially weaker than that for the ultrasmooth case on March 6, 1999, discussed above. The sequential soundings indicate that individual soundings on this day would be misleading and that the evolution and elimination of the stable internal boundary layer may be intermittent. As one possible explanation, accelerating flow above the thin, cool stable layer enhances the shear and induces mixing (boundary-layer recovery), which in turn reduces the shear and increases the Richardson number. This would lead to decay of turbulence and reformation of the cool stable layer adjacent to the surface. Unsteadiness of the upstream wind may also be a factor, particularly since the fetch at a given point is sensitive to wind direction.

7. Roughness Length Dependence on Stability

The aerodynamic roughness length generally decreases with increasing bulk Richardson number except for the most stable conditions (Figure 8). For the calculations in Figures 8 and 9, a lower threshold of 10^{-10} m was imposed on the roughness length to restrict the range of the vertical axis. Roughness lengths this small are probably zero within observational error. Therefore mean values in Figures 8 and 9 approaching 10^{-10} m

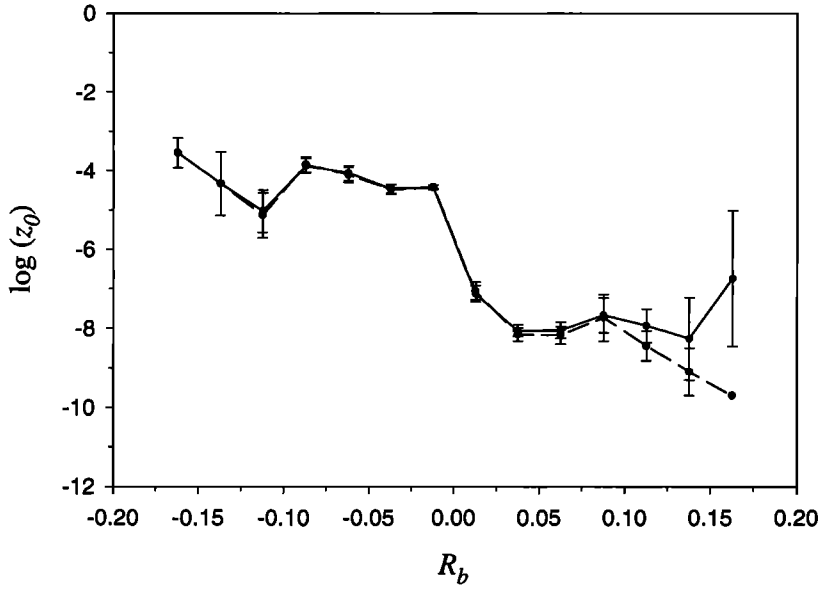

Figure 8. The dependence of the aerodynamic roughness length on the bulk Richardson number for November–December 1999 (solid line) and after removing cases with downward transport of vertical velocity variance (dashed line). Vertical brackets indicate the standard error.

imply that the roughness length is zero within observational error for many of the cases comprising the average.

Large values of the roughness length for very stable conditions occasionally occur with downward transport of vertical velocity variance toward the surface. Removal of these cases reduces the averaged value of the roughness length for very stable conditions, in which case the roughness length decreases with increasing stability. Since the turbulence in cases of downward transport of turbulence energy is not completely controlled by surface fluxes and z/L, Monin-Obukhov similarity theory may not apply. Then the aerodynamic roughness loses its physical meaning.

The roughness length (and the neutral drag coefficient) reaches a minimum value around 5 m s^{-1} (Figure 9), as is observed in numerous previous studies. This minimum value is thought to occur because of the combination of increasing roughness with increasing wind speed and special effects at weak winds. The special effects for weak winds include the role of surface tension and surfactants, transport by boundary-layer scale convective eddies, and "wave-induced" stress associated with swell.

We require that the stress vector be directed within 45 degrees of opposing the wind vector (section 3) to reduce the contribution of the swell to the composited roughness length.

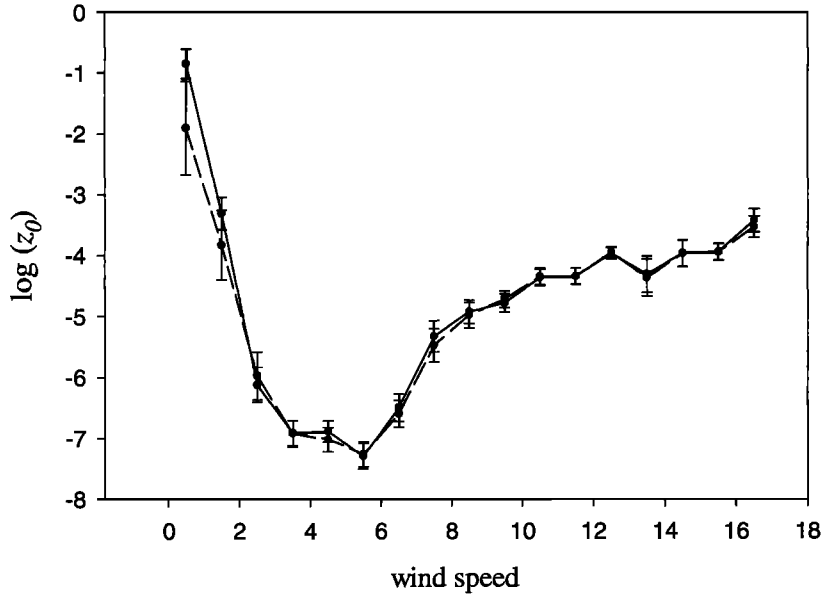

Figure 9. The dependence of the roughness length on wind speed for the November–December 1999 LongEZ data (dashed) and after removing restrictions on the stress direction (section 3) (solid). Vertical brackets indicate the standard error.

Relaxing this criteria (Figure 9, solid line) modestly increases the roughness length (and drag coefficient) at weak wind speeds but has little effect at other wind speeds. Therefore it is likely that part of the increase of the roughness length at weak wind speeds is due to wave-driven stress. The wave-driven stress is not expected to obey Monin-Obukhov similarity theory but enhances the stress and therefore the aerodynamic roughness length computed from that stress.

For weak wind stable conditions, longer waves exert an important influence on the stress, as was observed by *Plant et al.* [1999]. In fact, in their case the stress was nearly constant as the wind decreased to values below a few meters per second. *Rieder and Smith* [1998] find that the wave-induced part of the stress does not vanish as the wind vanishes, causing the drag coefficient to become large. However, they also find that even after attempting to remove the wave-driven stress, some increase of the drag coefficient at weak winds remains. *Mahrt et al.* [1996] found that the increase of the drag coefficient at weak wind speeds over the water is very sensitive to the method of calculation. *Mahrt et al.* [2001] show that the roughness length increases at weak winds speeds also over land surfaces, even over bare ground, alluding to meandering of the wind and stress vectors as a contributing factor.

These weak wind effects contribute to the dependence of the roughness length on stability since the stability tends to increase with decreasing wind speed. However, the present analysis (Figure 9) indicates that the roughness lengths are smallest for a combination of stable conditions and wind speeds in the range of 3–5 m s^{-1}. For winds greater than 6 m s^{-1}, the roughness length increases with increasing wind speed. This increase is due to near-neutral and unstable cases. The roughness length does not increase with wind speed for stable conditions.

8. Conclusions

The above analysis of LongEZ aircraft data and sonic anemometer data reveals frequent occurrence of very small surface stress and roughness lengths. These very small roughness lengths with near collapse of the turbulence are generally associated with advection of warmer air from land over colder water. Numerical estimates of the aerodynamic roughness length may be subject to large errors for weak surface fluxes in very thin boundary layers (section 3) because of significant random flux errors, systematic small-scale flux loss, errors due to fluctuations of the aircraft altitude, and errors in the estimated wind speed by the aircraft. With very thin, stable boundary layers, the stress may decrease significantly between the surface and the observational level. In this case, Monin-Obukhov similarity theory does not apply at the observation level, and the roughness length computed from the data must compensate for this inapplicability. Here "quasi-frictional decoupling" refers to very small values of the surface stress and roughness length and/or extremely thin atmospheric boundary layers. In spite of the above observational difficulties, the small values of the momentum flux inferred from the aircraft data also occur with sonic anemometer data collected from buoys and a tower at the end of a 570-m pier. Ultrasmooth values of the aerodynamic roughness length do not necessarily imply specific information on the wave state. The value of the aerodynamic roughness length only provides the correct flux given the specified stability functions (section 2), and its relationship to wave state in these cases is uncertain [*Sun et al.*, 2001].

The influence of warm air advection extends the influence of land off the coast for tens of kilometers or more. The very small roughness lengths for stable conditions are partly due to reduction of the downward momentum flux by the stable stratification. The data also show the usual minimum of the roughness length and neutral drag coefficient for wind speeds of about 5 m s^{-1}. The larger values of the roughness length at weaker wind speeds are partly associated with large deviations of the stress direction from opposite the wind vector, apparently due to the influence of swell. The very small roughness lengths are most likely to occur with a combination of intermediate wind speeds and stable stratification. Significant wind speed is required here to maintain the advection of warmer air over the cooler sea.

In some stable cases the vertical transport of turbulence may be downward, implying that the main source of turbulence is above the surface-based stable layer. In these cases the aerodynamic roughness length is much larger than that for the usual case of upward transport of turbulence energy. The multitude of physical influences on the surface stress and the difficulty of measuring weak momentum fluxes prevent categorical conclusions.

Acknowledgments. We gratefully acknowledge Jeff French, Ed Dumas, and Chris Vogel for important contributions to the three field programs. Will Drennen provided the data from the Romeo buoy. Bill Birkemeier and Gene Bichner of the U.S. Army Corps of Engineers Field Research Facility at Duck, North Carolina, are acknowledged for their helpful assistance. This material is based upon work supported by grants N00014-97-1-0279, N00014-98-1-0245, and N00014-97-F-0123 from the Office of Naval Research, Marine Meteorology.

References

Charnock, H., Wind stress over a water surface, *Q. J. R. Meteorol. Soc.*, *81*, 639–640, 1955.

Crescenti, G. H., T. L. Crawford, and E. J. Dumes, Data report: Long EZ(N3R) participation in the 1999 Shooling Waves Experiment (SHOWEX) pilot study, *Tech. Memo. ERL ARL-232*, Natl. Oceanic and Atmos. Admin., Silver Spring, Md., 1999.

Donelan, M. A., Air-sea interaction, in *Ocean Engineering Science*, edited by B. LeMehaute and D. M. Hanes, pp. 239–292, John Wiley, New York, 1990.

Dyer, A. J., A review of flux-profile relationships, *Boundary Layer Meteorol.*, *7*, 363–372, 1974.

Edson, J., and C. W. Fairall, Similarity relationships in the marine atmospheric surface layer for terms in the TKE and scalar variance budgets, *J. Atmos. Sci.*, *55*, 2311–2328, 1998.

Frederickson, P. A., and K. L. Davidson, Air-sea flux measurements from a buoy in a coastal ocean region, in *Fourteenth Symposium on Boundary Layers and Turbulence*, pp. 530–533, Am. Meteorol. Soc., Boston, Mass., 2000.

Freilich, M., and R. Dunbar, The accuracy of the NSCAT 1 vector winds: Comparisons with National Data Buoy Center buoys, *J. Geophys. Res.*, *104*, 11,231–11,246, 1999.

French, J. R., G. H. Crescenti, T. L. Crawford, and E. J. Dumas, Long EZ participation in the 1999 Shooling Waves Experiment (SHOWEX), *Data Rep. OAR ARL-20*, Natl. Oceanic and Atmos. Admin., Silver Spring, Md., 2000.

Geernaert, G. L., S. E. Larsen, and F. Hansen, Measurements of the wind stress, heat flux, and turbulence intensity during storm conditions over the North Sea, *J. Geophys. Res.*, *92*, 127–139, 1987.

Grachev, A., and C. Fairall, Upward momentum transfer in the marine boundary layer, *J. Phys. Oceanogr.*, *31*, 1698–1711, 2001.

Howell, J., and L. Mahrt, Multiresolution flux decomposition, *Boundary Layer Meteorol.*, *83*, 117–137, 1997.

Kahma, K., and M. Donelan, A laboratory study of the minimum wind speed for wind wave generation, *J. Fluid Mech.*, *192*, 339–364, 1987.

Kitaigorodski, S., and M. Donelan, Wind-wave effects on gas transfer,

in *Gas Transfer at Water Surfaces*, edited by W. H. Brutsaert and J. Jirka, pp. 147–170, D. Reidel, Norwell, Mass., 1984.

Maat, N., C. Kraan, and W. A. Oost, The roughness of wind waves, *Boundary Layer Meteorol.*, *54*, 89–103, 1991.

Mahrt, L., D. Vickers, J. Howell, J. Edson, J. Hare, J. Højstrup, and J. Wilczak, Sea surface drag coefficients in RASEX, *J. Geophys. Res.*, *101*, 14,327–14,335, 1996.

Mahrt, L., D. Vickers, J. Edson, J. Wilczak, J. Hare, and J. Højstrup, Boundary-layer transitions in offshore flow, *Boundary Layer Meteorol.*, *100*, 3–46, 2001.

Moller, D., P. Mourad, and S. Frasier, Field observations of radar backscatter from the ocean surface under low wind speed conditions, *J. Geophys. Res.*, *105*, 24,059–24,069, 2000.

Nordeng, T. E., On the wave age dependent drag coefficient and roughness length at sea, *J. Geophys. Res.*, *96*, 7167–7174, 1991.

Paulson, C. A., The mathematical representation of wind speed and temperature profiles in the unstable atmospheric surface layer, *J. Appl. Meteorol.*, *9*, 857–861, 1970.

Perrie, W., and B. Toulany, Fetch relations for wind-generated waves as a function of wind-stress scaling, *J. Phys. Oceanogr.*, *20*, 1666–1681, 1990.

Piccirillo, P., and C. Van Atta, The evolution of a uniformly sheared thermally stratified turbulent flow, *J. Fluid Mech.*, *314*, 61–86, 1997.

Plant, W., W. Keller, V. Hesany, K. Hayes, K. Hoppel, and T. Blanc, Measurements of the marine boundary layer from an airship, *J. Atmos. Oceanic Technol.*, *15*, 1433–1458, 1998.

Plant, W., D. Weissman, W. Keller, V. Hessany, K. Hayes, and K. Hoppel, Air/sea momentum transfer and the microwave cross section of the sea, *J. Geophys. Res.*, *104*, 11,173–11,191, 1999.

Rieder, K. F., and J. A. Smith, Removing wave effects from the wind stress vector, *J. Geophys. Res.*, *103*, 1363–1374, 1998.

Smedman, A.-S., H. Bergström, and B. Grisogano, Evolution of stable internal boundary layers over a cold sea, *J. Geophys. Res.*, *102*, 1091–1099, 1997a.

Smedman, A.-S., U. Hogström, and H. Bergström, The turbulence regime of a very stable marine airflow with quasi-frictional decoupling, *J. Geophys. Res.*, *102*, 21,049–21,059, 1997b.

Smedman, A., U. Hogström, and H. Bergström, The marine atmospheric boundary layer during swell, according to recent studies in the Baltic Sea, in *Air-Sea Exchange: Physics, Chemistry and Dynamics*, edited by G. L. Geernaert, pp. 175–196, Kluwer Acad., Norwell, Mass., 1999.

Sun, J., D. Vandemark, L. Mahrt, D. Vickers, T. Crawford, and C. Vogel, Momentum transfer over the coastal zone, *J. Geophys. Res.*, *106*, 12,437–12,448, 2001.

Toba, Y., and M. Koga, A parameter describing overall conditions of wave breaking, white capping, sea-spray production and wind stress, in *Oceanic Whitecaps*, edited by E. C. Monahan and G. Mac Niocaill, pp. 37–47, D. Reidel, Norwell, Mass., 1986.

Vickers, D., and L. Mahrt, Fetch limited drag coefficients over shallow water, *Boundary Layer Meteorol.*, *89*, 53–79, 1997a.

Vickers, D., and L. Mahrt, Quality control and flux sampling problems for tower and aircraft data, *J. Atmos. Oceanic Technol.*, *14*, 512–526, 1997b.

Vickers, D., and L. Mahrt, Observations of nondimensional shear in the coastal zone, *Q. J. R. Meteorol. Soc.*, *125*, 2685–2702, 1999.

Vickers, D., L. Mahrt, J. Sun, and T. Crawford, Structure of off-shore flow, *Mon. Weather Rev.*, *129*, 1251–1258, 2001.

Weissman, D., and H. Graber, Satellite scatterometer studies of ocean surface stress and drag coefficients using a direct model, *J. Geophys. Res.*, *104*, 11,329–11,335, 1999.

Wilczak, J. M., J. Edson, J. Højstrup, and T. Hara, The budget of turbulence kinetic energy in the marine atmosphere, in *Air-Sea Exchange: Physics, Chemistry and Dynamics*, edited by G. Geernaert, pp. 153–174, Kluwer Acad., Norwell, Mass., 1999.

Winstead, N., and G. Young, An analysis of exit flow drainage jets over the Chesapeake Bay, *J. Appl. Meteorol.*, *39*, 1269–1281, 2000.

T. L. Crawford and G. Crescenti, NOAA Air Resources Laboratory, Idaho Falls, ID 83402, USA.

P. Frederickson, Naval Postgraduate School, Monterey, CA 93943, USA.

L. Mahrt and D. Vickers, College of Oceanic and Atmospheric Sciences, Oregon State University, Corvallis, OR 97331, USA. (mahrt@oce.orst.edu)

J. Sun, National Center for Atmospheric Research, Boulder, CO 97331, USA.

(Received November 13, 2000; revised May 18, 2001;
accepted May 21, 2001.)